Flowline Variations in Abyssal Hill Morphology for the Pacific-Antarctic Ridge at 65° S

Ana Macario[1], William F. Haxby
Lamont-Doherty Earth Observatory, Palisades, New York

John A. Goff
University of Texas Institute for Geophysics. Austin, Texas

William B. F. Ryan
Lamont-Doherty Earth Observatory, Palisades, New York

Steve C. Cande
UCSD, La Jolla, California

and Carol A. Raymond
JPL, Caltech, Pasadena, California
Jet Propulsion Laboratory

Bouguer gravity anomalies, (3) Toward the segment ends 1 I estimates arc 27-68% larger while λ estimates either do not significantly change (to the north of the PFZ) or are up to 40% smaller (to the south of the PFZ). Wc speculate Urat these H and λ changes seen toward the segment ends are related to either an increase in the amount of extension (without a corresponding increase in the strength of the lithosphere) or variations in the relative contribution of constructional volcanism to overall abyssal hill morphology. One might expect that detachment surface tectonics would play an important role in abyssal hill creation during the slower spreading interval. However, the sense of asymmetry in abyssal hill size is opposite to the predictions of the model. Furthermore, contrary to the detachment model predictions, there is no asymmetry in apparent crustal thickness for this period, (Abyssal hill morphology, Pacific-Antarctic ridge, intcnncdiatc-spreading rates, mantle Bouguer gravity anomalies)

INTRODUCTION

Abyssal hills arc created at divergent plate boundaries by extensional tectonics and constructional volcanism. Though modified by off-axis volcanism, sedimentation and mass wasting, they represent an indirect record of the complex dynamics of mid-ocean ridge processes. Previous studies [Menard, 1967; Goff, 1991; Hayes and Kane, 1991; Malinverno, 1991 and Goff, 1992] have demonstrated a negative correlation between abyssal hill size parameters and the spreading rate (up to -100 mm/yr) of the mid-ocean ridge at which they were formed. There arc two postulated cause.s for this correlation: (1) variations in axial thermal structure as a function of spreading rate; cooler lithosphere at slower rates will be able to elastically support larger surface loads as well as larger normal faults [e.g., Goff, 1992]; and (2) the change from axial valley morphology at slower rates to axial high at faster rates (at approximately 70 mm/yr [Small and Sandwell, 1989]); the axial valley generates large (up to 1 km throw) inward-facing normal faults which, after likely back tilting over adjacent rift mountains, arc preserved in the abyssal hill record [e. g., Macdonald, 1982]. More recently, numerical models for crustal genesis have suggested that variations in crustal thickness may also significantly affect the heat budget and indirectly the ridge crest morphology [Phipps Morgan and Chen, 1993]. For the Mid-Atlantic ridge, a negative correlation between abyssal hill size parameters and crustal thickness inferred from mantle Bouguer gravity anomalies was proposed by Goff et al. [1992] and Lin et al. [1992].

A recent geophysical survey centered on the Pitman Fracture Zone, PFZ (Ewing cruise 92-1; Cande et al. [1992]; Haxby et al. [1992]) acquired high-resolution bathymetry, gravity and magnetic data along a 60 km-wide corridor extending to 12 Ma to either side of the Pacific-Antarctic ridge flanks at 65°S (see Figure 1 for cruise location). The data coverage along the two adjacent ridge segments provides an excellent opportunity to evaluate the dynamical evolution of this intermediate-spreading rate ridge as constrained by the abyssal hill record. The relative dependence of off-axis abyssal hill morphology on the temporal and spatial variations in spreading rate and crustal thickness (as inferred from mantle Bouguer gravity anomalies) is examined in this study. We use methodology of Goff and Jordan [1988] to characterize the second-order statistics of abyssal hill morphology. The main assumption of their method is that seafloor can be modeled as an approximately stationary anisotropic random field defined in part by a parameterized functional form of its covariance function. Standard techniques are used to estimate spreading rates and mantle Bouguer gravity anomalies. Three questions arc addressed in this study: (1) what arc the systematic flowline variations in abyssal hill morphology?, (2) arc there variations in abyssal hill morphology that cannot be attributed to the spreading rate dependence?, and (3) does the morphology vary systematically with other indicators of varying axial thermal structure (i.e., mantle Bouguer gravity anomalies)?

The primary size and shape of abyssal hills is controlled by a complex combination of tectonic (normal faulting) and constructional (volcanism) processes operating at or near the ridge-axis. Volcanism contributes to the axial relief by either creating constructional edifices (typically at slow-spreading ridges) [e.g., Lewis, 1979; Kong et al., 1988; Kappel and Ryan, 1986; Pockalny et al., 1988; Smith and Cann, 1990] or by modifying the existing terrain by flooding bathymetric lows or spilling down existing slopes (typically at fast-spreading ridges) [e.g., Keeley et al., 1992; Goff et al., 1993]. Alternatively, vertical (inflation-deflation of the axial magma chamber) [Edwards et al, 1992] and/or horizontal (lithospheric extension) [e.g., Lonsdale, 1977] forces are thought to induce abyssal hill formation by normal faulting at both slow and fast-spreading ridges [e.g. Rea, 1975; Lonsdale, 1977; Harrison and Stieltjes, 1977; Macdonald and Atwater, 1978; Bicknell et al., 1987; Carbotte and Macdonald, 1991]. We take the view that constructional edifices, sheet flows and normal faulting combine to create of abyssal hill morphology,

In this paper, we first present the results of the statistical characterization study using the most robust abyssal hill size parameters (RMS height H and characteristic width λ). The flowline variations in H and λ estimates are then compared to the spreading rate history and the mantle Bouguer gravity anomalies. In general, we find that both H and λ are negatively correlated to spreading rate. Flowline variations in λ estimates over regions of approximately uniform crustal thickness may be interpreted, in the context of the normal faulting theory of Malinverno and Cowie [1993], as an indication of episodic changes in the lithospheric strength in the vicinity of the ridge crest. It also follows from their theory that an increase in the amount of extension (without significant changes in the flexural rigidity) may explain the increase in H accompanied by no than.gcs in λ toward the northern segment end. However, we cannot currently rule out that the overall lack of systematic variations in λ (estimates either do not significantly change or decrease toward the northern and southern segment ends respectively) may be related to constructional volcanism. In contrast with previous studies on the flanks of the Mid-Atlantic Ridge, the abyssal hill size estimates presented here are not strongly correlated with crustal thickness (as inferred from mantle Bouguer gravity anomalies). Remarkable exceptions to the negative relationship between abyssal hill size parameters and spreading rates are found in this study. Processes occurring during or shortly after abyssal hill formation (e.g. plate reorganizations induced by far-field stresses) may partially account for some of the morphological asymmetries seen for opposite ridge flanks and across the PFZ.

PACIFIC-ANTARCTIC RIDGE AT 65 ° S - BACKGROUND INFORMATION

The free-air gravity map derived from Geosat/Seasat altimeter data for the studied area and surroundings is shown in Figure 1. The box shows the location of the 60 km wide by 600 km long corridor for which we have full Hydrosweep, magnetic and gravity data coverage. The two adjacent segments currently spreading at -56 mm/yr [Cande et al., 1992] are offset by a -70 km long right stepping transform. The transition from a rift valley (south of the PFZ) to an axial high (north of the PFZ) is inferred based on the observed change in the axial gravity signal. The portion of the Pacific-Antarctic ridge associated with the rift valley is also characterized by an unusually small subsidence constant relative to global averages [Marks and Stock, 1994].

Figure 2 shows the gridded bathymetry, magnetic and mantle Bouguer gravity anomaly data. In order to facilitate the discussion of the results, we will apply the terms "Pacific north" and "Pacific south" to refer to the portion of the Pacific plate situated to the north and south of the PFZ respectively. A similar rationale applies to the Antarctic plate. Due to limited data coverage on the Antarctic plate (restricted to a narrow band close m the PFZ), we have carried out our analysis only to the portion situated to the north of the PFZ (Antarctic north). The northern and southern ridge segments overlap by 5 km and their respective tips are curved towards the transform. This portion of the Pacific-Antarctic ridge is also characterized by the presence of curved abyssal hill tips only on the outside corners (analogous to "hooked ridges" defined by Fornari et al. [1989]). The mantle Bouguer gravity anomaly map reflects deviations from the assumed simple model of constant crustal thickness and density, and variations in mantle density associated with its theoretical thermal structure. The transition from an axial high to a rift valley coincides with an apparent thinning of the crust from north to south across the PFZ. Although we do not observe a rift valley within the surveyed area, the ridge axis to the south is deeper.

The late Neogene spreading rate history for the Pacific-Antarctic ridge is illustrated in Figure 4a based on the anomaly identification by Cande et al. [1992]. The most prominent feature of the spreading history is a sharp acceleration at Chron 3ay (5.8 Ma using the Cande and Kent [1992] geomagnetic polarity time scale) from -40 mm/yr to -60 mm/yr. Ridge-axis jumps, deduced from a preliminary analysis of bathymetry and magnetic data [Ryan et al., 1992] may explain part of the highly variable (both in direction and magnitude) asymmetric spreading history of this ridge (Figure 4b-c).

STOCHASTIC CHARACTERIZATION

The methodology used to characterize the second-order statistics of abyssal hill morphology and the inversion procedure arc presented in Goff and Jordan [1988]. The analyses were performed on three Hydroswccp swaths to the north of the PFZ and two swaths to the south (the furthest ones from the PFZ). Uncertainties in the estimation of some parameters (i.e., fractal dimension and aspect ratio [Goff, 1991]), caused us to focus our analysis on the most robust second-order statistics: (1) RMS height, H, the average variation of bathymetry about the mean depth, and (2) characteristic width, λ, roughly the average peak-to-peak distance between the most prominent peaks obtained from the width of the covariance function in the normal-to-strike direction. Although normal faulting is important in the formation of abyssal hills, λ dots not necessarily reflect the width of a single faulted block, but rather the average spacing between the main topographic highs or lows.

Our principal assumption is that variations in off-axis abyssal hill statistics arc primarily related to temporal changes in the axial processes (faulting and volcanism) which generate abyssal hills. However, secondary processes such as off-axis volcanism, sedimentation and mass-wasting, can modify the statistical characteristics of abyssal hills. For the study area, wc have enough evidence to assume that these processes have not caused major changes in abyssal hill morphology. Visual inspection of the echosounder records reveals a very thin sediment cover in the older portions of the studied area together with negligible signs of mass-wasting. To avoid the effect of off-axis volcanism, wc have intentionally excluded from the analysis the region of the Antarctic plate north of the PFZ where the only clear evidence of secondary flood basalts exists (O-2 Ma old crust).

In order to assure well-resolved abyssal hill size parameters, the swaths of multibeam data used as input must have a length -8-10 times the characteristic abyssal hill width. For intermediate-spreading ridges, the characteristic widths range from 3-7 km [Goff, 1991]. In addition, it is essential that the portion of the seafloor to be analyzed consists principally of abyssal hill morphology. In this study wc visually identify three areas that do not satisfy this criteria (Figure 2): (1) a 'visually' smooth spot (resembling outpouring of off-axis volcanism) found on the Antarctic plate to the north of the PFZ for crustal ages between ()-2 Ma; no swaths were taken across this area, (2) prominent seamounts found on the Pacific plate for crustal ages less than 4 Ma; the seamounts were excluded from the analysis, and (3) a large topographic high (bulge) spanning crustal ages between 8-10 Ma present on the northern Pacific plate that was formed by processes different from the ones related to abyssal hill formation; in order to avoid this feature which clearly departs from the normal cooling curve, only the northernmost swath was used.

A set of obliquely trending cracks overprinting the abyssal hill fabric is found on the Pacific plate to the north of the PFZ for crustal ages between 6-8 Ma. For this particular case wc fixed the characteristic length and orientation of the peculiar fabric to values similar to the adjacent seafloor in order to obtain stable H and λ estimates. Once the inversion parameters arc obtained, the fit of the model covariance to the estimated covariance was systematically used to assess how successfully the parameters were estimated.

The process of choosing the swath segments, including avoidance of the terrains stated above is unavoidably subjective. In addition to the abyssal hill criteria, wc must also balance between swath segments which arc long enough to resolve parameters, yet short enough to resolve spatial variations (inhomogeniety). Large, well-defined scarps in the midst of smaller abyssal hills along the northern segments between 4-6 Ma arc an obvious example (wc apply the term locally "anomalous" seafloor fabric to such terrain). The presence of such large scarps bounding the swath segments is sufficient to cause a significant increase in both H and λ values relative to surrounding seafloor as they will tend to dominate the covariance function. It is precisely this type of change in morphology that we wish to quantify.

The swaths used in this study were fragmented into 50-80 km long segments, which limits our temporal resolution at these spreading rates to 1-2 Ma. In the worst possible scenario, if a ridge-axis jump of the order of 5 km has occurred, a maximum of 10% of the total length of any given swath segment would be compromised, Most of the swaths used in this study were -17-40 km away from the PFZ. In order to investigate the fracture zone influence on abyssal hill morphology, an additiona swath analysis was carried out along flowlines adjacent to the PFZ (-5 km).

ABYSSAL HILL Characterization - RESULTS

Flowline Variations

The results of individual analyses as a function of age arc displayed in Figure 5. For ages between O and 4 Ma (O-6 Ma for the Pacific south) the well-resolved RMS height estimates are remarkably uniform. Estimates for older crust (8- 12 Ma) show larger uncertainties and scatter. Although the characteristic width estimates show a similar trend for the Antarctic plate, the differences in λ uncertainties between young and old seafloor arc not so pronounced for the Pacific plate. Table 1 shows the weighted average estimates of the RMS height and characteristic width. These average estimates were obtained by grouping the original parameters into 2 Ma old bins and then weighting them by the inverse of their variance [Goff and Jordan, 1989]. The standard deviation of the parameters are reported in Table 1 along with 1σ standard deviation on the weighted average arc calculated as described in Goff [1991]. While the tabulated uncertainty values represent the resolution of the weighted average, the standard deviation expresses the scatter of a particular parameter.

The significance of the change in abyssal hill size parameters between young (O-4 Ma) and old (>8 Ma) crust can be assessed by examining the weighted averages and their variances. The variance of the difference of two uncorrelated estimates is the SUM of the variances of each estimate. Hence the significance of the difference between two weighted averages can be easily established. For the Antarctic north, both RMS height and characteristic width estimates obtained for crustal ages less than 4 Ma are smaller than estimates for crustal ages greater than 8 Ma. The difference is approximately 5 times the square root of the standard deviation of the estimates, so the change in abyssal hill characteristics on that flowline arc wc]] resolved at greater than 99.9% confidence. For the Pacific plate, while the decrease in RMS height is very well resolved (99% confidence for the Pacific north and 95% for the Pacific south), the decrease is characteristic width is less significant (less than 68% confidence in both cases). These confidence limits indicate that the hi-modal character of H estimates (small values for young crust and large ones for old crust) is very well resolved for troth Antarctic and Pacific plates while for λ estimates it is only well resolved for the Antarctic plate.

For crustal ages between 0-4 Ma, RMS height and characteristic width estimates arc similar across the PFZ (the small differences arc not statistically significant). In addition, results for the flowlines to the north of the PFZ indicate a remarkable symmetry in abyssal hill size parameters for opposite ridge flanks. However, H and λ estimates for crustal ages between 4-6 Ma arc significantly higher for the flowlines to the north of the PFZ. This corresponds to the age range where the locally "anomalous" terrain defined above is visually recognized (large well defined scarps in the midst of smaller abyssal hills). A well resolved difference in the RMS height and characteristic width between the Pacific north and Antarctic north flowlines is observed for isochrons in the 8-12 Ma range. Abyssal hills along the Antarctic north flowline arc on average 47 m taller and 2 km wider than those along the Pacific north flowline in the same age range.

Table 1 also illustrates the differences in the averaged weighted estimates between swaths taken adjacent (-5 km) and away (-1-1-40 km) from the PFZ. For all subareas, wc find significantly larger estimates of H (by 25-58 m) near the PFZ relative to the estimates obtained for the swaths taken away from the PFZ. Although no significant changes in characteristic width estimates arc observed to the north of PFZ, λ is smaller near the PFZ for the Pacific south (by 2.2-2.4 km).

Relationship With Spreading Rate

The negative relationship between the binned abyssal hill size parameters and the spreading rate history is illustrated in Figure 6. The negative Pearson's correlation coefficient, R, and estimated confidence, C [Press et al, 1991] between H estimates and full spreading rates arc high for all subareas when the locally "anomalous" seafloor fabric is excluded from the regression analysis (R=-O.93, -0.96 and -0.99 and C=96, 97 and 99% for Antarctic north, Pacific north and Pacific south respectively; Figure 6a). The degree of correlation between λ estimates and full spreading rate is also high (R=-0.85, -0.83 and -0.85 and C=94, 94 and 96% for Antarctic north, Pacific north and Pacific south respectively; Figure 6b). The anomalous character of the seafloor fabric for 4-6 Ma old crustal ages is clearly documented here as a deviation from the negative trend between abyssal hill size parameters and spreading rates (correlation coefficients arc smaller when the locally "anomalous" fabric is included). The negative correlation between abyssal hill size parameters and full spreading rate averaged for the three subareas is shown in Figure 6c-d as regional averages. When the locally "anomalous" estimates arc excluded, the correlation coefficients and confidence limits between spreading rates and abyssal hill size parameters arc R=-0.99, C=97% for H estimates and R=-0.93 and C=96% for λ estimates. Wc have also plotted in Figure 6c-d the weighted estimates obtained for swaths adjacent to the PFZ (averaged for the three subareas; binned weighted estimates for individual subareas arc shown in Table 1). The RMS height averages in this case clearly plot above the local trend.

Figure 7a demonstrates a well-rcso]vcd high positive correlation between RMS height and characteristic width (R=0.97, 0.95 and 0.89 and C=98, 98, and 97% for Antarctic north, Pacific north and Pacific south respectively). The correlation coefficient between RMS height and characteristic width estimates averaged for the three subareas is high at high confidence levels (R=0.92 and C=98%; Figure 7b). The weighted estimates obtained for swaths adjacent to the PFZ once again slow a clear departure from the regional trend.

DISCUSSION AND INTERPRETATION

The main assumption in this study is that off-axis abyssal hills represent an indirec record of the axial processes (faulting and volcanism) which created them and thus provide an excellent opportunity to quantify temporal variations in the dynamics of mid-ocean ridge processes. The flowline variations in H and λ estimates suggested by this study (Figure 6) demonstrate that abyssal hills formed during slower spreading periods are significantly larger than hills created during the faster spreading interval. However, some noticeable exceptions to this spreading rate dependence arc present: (1) the locall y "anomalous" character of abyssal hill fabric found for crusts] ages in the 4-6 Ma age range for northern segment flowlines, (2) the significant asymmetry in abyssal hill morphology at older ages for opposite northern ridge flanks, and (3) the changes in abyssal hill size estimates near the axial discontinuity. In this discussion, wc consider these deviations in abyssal hill morphology in terms of crustal thickness variations (as inferred from mantle Bouguer gravity anomalics) and largc scale plate stresses.

Correlation with Spreading Rate

Mid-ocean ridges spreading at full rates <36 mm/yr arc generally characterized by the presence of a rift valley 1-2 km deep and 15-20 km wide [e.g. Macdonald, 1984]. Average abyssal hill RMS height and characteristic width parameters obtained for the Mid-Atlantic Ridge (full rates: 20-36 mm/yr) arc 197 m and 7.1 km respectively [Goff, 1991]. Values of H and λ for abyssal hills generated at fast-spreading ridges (>65 mm/yr) arc significantly smaller (56 m and 2.0 km respectively [Goff, 199 l]). Fast-spreading ridges arc generall y characterized by an axial high 100-200 m high and 1-2 km wide [e.g. Macdonald, 1982]. Modeling efforts [Chen and Phipps Morgan, 1993] together with gravity studies [Small and Sandwell, 1989] indicate that the transition from an axial valley and m an axial high is abrupt. Based on topographic evidence, Malinverno [1993] suggests that for a fixed axial depth, spreading rate variations as small as 15 mm/yr arc enough to trigger a change from an rift valley to an axial high.

The primary result of this study is that abyssal hill size characteristics arc negatively correlated with spreading rate (Figure 6), in agreement with the results of previous studies [Menard, 1967; Goff, 1991; Malinverno, 1991; Hayes and Kane, 1991 and Goff, 1992]. In particular, wc find that during slower spreading periods (ages >8 Ma; full rates: 36-44 mm/yr), abyssal hill estimates arc 31-86% taller and 21 ->100% wider than during the faster spreading intervals (ages <4 Ma; full rates: 52-63 mm/yr range). Figure 8 illustrates the complex relationship between abyssal hill morphology and spreading rate based on a compilation of abyssal hill size parameters given in Goff [1991]. An increase in both RMS height and characteristic width as spreading rates decreases is ob.served. However, the very fmt-spreading rate data (Pacific-Nazca, PN) displays slightly larger abyssal hill size parameters than the fast-spreading rate data (Pacific-Cocos, PC). There is a good a good agreement between the abyssal hill size parameters proposed by this study for O-2 Ma (full rates -55 mm/yr), and the and the ones found for the Pacific-Rivera and African-Indian subsets (PR+AI). For abyssal hills created during slower spreading periods (10-12 Ma, full rates -39 mm/yr), H and λ estimates arc in between the values found for the Mid-Atlantic Ridge (MAR) and PR+PI.

Onc likely mechanism for this negative correlation between abyssal hill size and spreading rate is the variation in axial thermal structure associated with spreading rate: a cooler lithosphere implied for slow-spreading ridges has a thicker elastic core and thus is able to support larger abyssal hills, and larger normal faults associated with abyssal hills [e.g., Forsyth, 1992]. In contrast, the thinner elastic layer resulting from higher ridge crest temperatures in the vicinity of fast-spreading ridges allows only small abyssal hills and small normal faults to be supported. Given the spreading rate variability documented for the study area between the older and younger portions of the seafloor (full spreading rates range from 36 to 63 mm/yr) it is reasonable to expect that the axial topography is reflecting the variability in the axial thermal structure. Rift valleys arc accompanied by very large inward-facing faults which, after back-tilting over the rift mountains, arc preserved as abyssal hill structures [e. g., Macdonald, 1982]. Mid-ocean ridges with axial highs do not undergo this form of intensive tectonism. It is therefore likely that sornc component of the negative relationship between abyssal hill size properties and spreading rate is related to the transition from axial valley to axial high morphology.

H and λ Relation

According to the theoretical formulation for topographic roughness due to normal faulting proposed by Malinverno and Cowie [1993] the characteristic width of a faulted block is controlled by the flexural wavelength. Their formulation assumes the lithosphere behaves like an elastic plate, faults have a vertical dip and infinite length, faults do not interact and fault parameters and locations represent independent variables. According to the theory of Malinverno and Cowie [1 993], the variation in λ estimates seen in Figure 5 can bc explained in terms of flowline changes in the strength of the lithosphere in the vicinity of the ridge crest (wider fault blocks arc formed during slower spreading periods when the, lithosphere is elastically stronger). These predictions are in good agreement with inferred variations in flexural rigidity based on the spreading rate history shown in Figure 4a.

The positive correlation between abyssal hill size parameters shown in Figure 7 dots not contradict the functional relationship between H and λ that is predicted by an extension of the normal fault theory of Malinverno and Cowie [1993] (H proportional to $\sqrt{\lambda}$; Malinverno personal communication). A similar positive trend is also expected to develop as a result of constructional volcanism. i.e., taller volcanic edifices arc also expected to bc wider from simple isostatic principles [Vogt, 1974]. However, due to difficulties in constraining model parameters (e.g. Malinverno [1991]), no predictions on the topographic roughness due to constructional volcanism have been put forth. To date, only qualitative statements can bc rnadc such as abyssal hills generated at slow-spreading portions of the Mid-Atlantic Ridge also tend to have a positive correlation between H and λ, whereas those generated along fast-spreading portions of the East Pacific Rise tend toward either a negative or zero correlation between H and λ [Goff, 1991; Goff et al., 1993]. In this respect the intermediate spreading rate abyssal hills within the survey bear more morphological resemblance to those generated at slow-spreading ridges.

Correlation with Mantle Bouguer Gravity Anomaly

Axial thermal structure and morphology arc not independent variables. Numerical models for crustal genesis that incorporate hydrothermal cooling and crustal accretion by means of magma lenses have recently attempted to explain the long-established spreading rate dependence of ridge crest morphology [Phipps Morgan and Chen, 1993]. This model also incorporates the effect of variation in crustal thickness into the heat budget. According to their results, the axial thermal structure, which depends on both spreading rate and magma input, exerts control on the ridge crest morphology. Given this suggested relation between crustal thickness and morphology, it is reasonable to expect that seafloor regions underlying by thinner crust arc likely to be associated with a stronger lithosphere (due to the greater proportion of mantle rocks which arc rheologically stronger than crustal rocks) which in turn is able to support larger abyssal hills.

Crustal thickness variations inferred from mantle Bouguer gravity anomalies at slow-spreading ridges have been used to suggest that abyssal hill morphology is controlled by the axial temperature structure and/or deep melt supply [Goff et al., 1992; Lin et al., 1992]. These studies demonstrate a negative relation between magnitude of the crustal thickness (inferred from mantle Bouguer gravity anomalies) and abyssal hill size. For this study area, the positive mantle Bouguer gravity anomaly to the south of the PFZ (interpreted as thinner crust) is not accompanied by a corresponding increase in abyssal hill size parameters (Figures 2c and 5). We did not find evidences for a systematic relationship between flowline variations in abyssal hill size and mantle Bouguer gravity anomalies (i.e., the taller and wider abyssal hills found for crustal ages > 8 Ma arc not associated with more positive mantle Bouguer gravity anomalies). Furthermore, despite the large difference in abyssal hill size parameters across the ridge axis for crustal ages > 8 Ma, no significant asymmetry in the mantle Bouguer gravity anomalies arc detected. "

In summary, we find no systematic evidence for a negative relation between abyssal hill size parameters and mantle Bouguer gravity anomalies for the Pacific-Antarctic ridge. We suggest that for intermediate-spreading ridges either the inferred crustal thickness control on abyssal hill morphology is much more complex than as demonstrated for slow-spreading ridges or that the variations in the mantle Bouguer gravity anomalies arc not representative of the true crustal thickness. The latter possibility arises from recent studies which have questioned the validity of using mantle Bouguer gravity anomalies to infer crustal thickness variations for fast-spreading ridges and offered alternative explanations for the bull's eyes pattern often seen at slow-spreading ridges [Mutter and Karson, 1992; Wang and Cochran, 1993].

"Anomalous" Seafloor Fabric

The locally "anomalous" 4-6 Ma old seafloor fabric found for the flowlines to the north of the PFZ coincides with the last major increase in spreading rates (Chron 3ay) and clockwise changes in abyssal hill lineaments of -1O°. However, it is hard to establish a causal relationship between this local morphological anomaly and variations in spreading magnitude and direction over a short period of time. An analysis of the gravity field surrounding the surveyed area (Figure 1) suggest the presence of topographic features indicative of recent changes in the stress field. Examples of such features area propagating rift and a relict fracture zone located to the north of the PFZ. The oblique lineations found only on the northern Pacific plate for 6-8 Ma old crustal ages reprc.sent another set of topographic features indicative of changes in the stress field. Wc do not currently understand what caused either the locally "anomalous" crustal fabric at 4-6 Ma or the oblique lineations. The fact that the former is observed only to the north of the PFZ and the latter only for onc ridge flank (Pacific north) may imply asymmetric far-field forces. Wc speculate that spatial and temporal asymmetries in the regional stress field across the PFZ and across the ridge axis may partially account for some of the morphological discrepancies shown here.

lnsidc/Outside Corner Asymmetries

Based on multichannel seismic reflection profiling and deep drilling results for oceanic crust, Mutter and Karson [1992] proposed a structural model for slow-spreading ridges in which low angle normal faults (footwall detachment surfaces) dip obliquely to the spreading direction towards the ridge-transform intersection. According to this model, the inside corner "detachment surface" is broken up by high-angle normal faults. Although no direct abyssal hill size predictions can be made based on this model, wc speculate that the inside corner should support larger abyssal hills if it is characterized by a stronger lithosphere relative to the outside corner (greater crustal extension associated with the inside corner leads to a greater proportion of mantle rocks; these in turn are rheologically stronger than crustal rocks resulting in higher lithospheric strength relative to the outside corner).

The prediction of a thinner crust and, indirectly, larger abyssal hills for the inside corner has been recently supported by side.scan, bathymetry and gravity data on the Mid-Atlantic Ridge at 25-27° N [Tucholke et al., 1992]. However, in the slower spreading portion of this study area (ages >8 Ma; full rates 36-44 mm/yr), no systematic inside/outside corner asymmetries in crustal structure arc observed (as inferred from the mantle Bouguer gravity anomaly; Figure 2c). In the faster spreading portion (ages < 4 Ma; full rates 52-63 mm/yr) some asymmetry in crustal thickness is observed to the north of the PFZ, but it is variable and can be related to volcanic overprinting. At crustal ages >8 Ma, there is a large inside/outside corner asymmetry in estimates of H and λ to the north of the PFZ but it is in the "wrong" sense, i.e., abyssal hills found on the Antarctic plate (outside corner) arc significantly larger than those on the Pacific plate (inside comer) (Figure 5; Table 1). Note that different half-spreading rates across the ridge axis to the north of the PFZ (Figure 4b) also fail to explain this asymmetry. At younger ages there is no significant asymmetry in abyssal hill characteristics. In this respect, the studied portion of the Pacific-Antarctic Ridge has a morphological/structural behavior more similar to a fast-spreading ridge (no systematic inside/outside corner asymmetries) than a slow-spreading ridge.

Morphological inside/outside corner asymmetries may also develop as a result of ridge-axis jumps. According to Palmer et al. [1993], asymmetrical splitting of the axially elongated volcanic edifices seen along the Antarctic Australian Discordance (intermediate-spreading portion of the Southeast Indian ridge) due to ridge axis jumps provides a mechanism for creating morphological asymmetries for opposite ridge flanks. For the case of the study area where ridge-axis jumps arc thought to occur [Ryan et al, 1992], the similarity in abyssal hill size parameters to the north of the PFZ across the ridge axis (crustal ages < 8 Ma) can be attributed to random ridge axis jumps (both in magnitude and direction) over a short time scale. In this case wc would have an equal probability of finding the taller and wider portion of the split volcanic construction on both sides of the ridge. These random ridge-axis jumps may provide a mechanism for creating abyssal hills with similar size range across the ridge axis.

Proximity to the Pitman Fracture Zone

This study indicates that toward the segment ends H estimates arc systematically larger while λ estimates either do not significantly change (to the north of the" PFZ) or arc up to 40% smaller (to the south of the PFZ) (Table 1). The increase in H near the PFZ is in agreement with previous statistical studies on abyssal hill morphology of the fast-spreading northern East Pacific Rise [Goff, 1991] and southern East Pacific Rise [Goff et al., 1993]. Shaw [1992] also found an increase in throw and spacing of faults near segment ends along the slow-spreading Mid-Atlantic Ridge between Kane and Atlantis fracture zones.

In the context of the normal faulting model of Malinverno and Cowie [1993], the observations to the north of the PFZ can be interpreted as an increase in the amount of extension (the product $\varphi\langle h^2 \rangle$ in their formulation) without a corresponding significant increase in the flexural rigidity. Such scenario is in agreement with Goff [1991] predictions of a larger volume of extensional deformation at ridge segment ends based on Chen and Morgan [1990] numerical experiments. An additional consideration is that the more robust and steady-state magma supply toward the segment midpoint will cause volcanic flooding of topographic lows. This smoothing effect will decrease H estimates and possibly result in the larger λ estimates we observe away from the fracture zone in the south flowlines.

Most of the variability in abyssal hill size parameters shown in this study occurs along flowlines and a strong positive correlation between H and λ is observed (Figure 7). In contrast, a negative or flat correlation between H and λ estimates is present near segment ends as shown by the decrease or constancy in λ, and increase in H, toward the PFZ (Figure 7c-d; Table 1). If this negative or flat trend is an effect of ridge segmentation, then we speculate that abyssal hill variations associated with ridge segmentation occur by different mechanisms than those associated with temporal variability in mid-ocean ridge dynamics. We suggest that variations in abyssal hill parameters associated with ridge segmentation arc caused by the interplay between relative contributions of extensional tectonism and constructional volcanism (correlation bctwccn H and λ will depend on the relative importance of each mechanism). In contrast, wc believe that temporal changes in abyssal hill parameters arc duc to variations in predominantly just onc of these processes (resulting in a positive correlation between H and λ estimates).

Topographic Roughness

Malinverno [1990] developed a roughness-length method which consists of breaking up a profile in windows of varying lengths and calculating the average roughness for any given window length. Like the power spectral density, the roughness-length relationship follows a power law distribution for wavelengths less than a factor proportional to the characteristic flexural length scale α. Using independent estimates for fault scarp height, fault spacing and flexural wavelength, Malinverno and Cowie [1993] found that normal faulting can account for all the observed topographic roughness of the East Pacific Rise (15° N-14° S). Although such independent estimates arc not available for the study area, the "roll-off" point (break in the power law behavior) in a roughness vs. window length graph can bc used to make inferences on the average flexural strength of the lithosphere. Specifically, it follows from the formulation of Malinverno and Cowie [1993] that for window lengths greater than 2.8a, the average predicted roughness is a constant independent of the window length. Alternatively, for window lengths less than 2.8α, the average predicted roughness is proportional to the square root of the window length (power-law holds in this case). In Figure 9a, the dots represent the observed topographic roughness (obtained using the roughness-length method) for two -1350 km long flowlines extending out onto -40 Ma on either side of the adjacent ridge segments. For the segment to the south of the PFZ, the "roll-off" from the power-law regime to a hat line happens at larger window lengths than for the segment to the south of the PFZ. The formulation of Malinverno and Cowie [1993] predicts that the characteristic flexural wavelength scale for the southern ridge segment (α -22 km; Te -5.6 km) is larger than the northern one (α -11 km; Te -2.1 km) and therefore that the lithosphere created at the southern ridge segment is on average stronger than the northern segment. This inferred change in flexural strength is in agreement with the presence of a rift valley to the south of the PFZ and an axial high to its north, as seen on the satellite-derived free-air gravity map of Figure 1. Figure 9tr illustrates the power spectral density for" the same flowlines used in topographic roughness analysis. We note that for almost all wave numbers the southern segment has in average more topographic power than the northern one (except in the 0.2-0.5 km^{-1} range)."

SUMMARY AND CONCLUSIONS

We presented here the results of a statistical characterization study of the abyssal hills formed by two adjacent intermediate-spreading rate segments. The two most robust abyssal hill size estimates (RMS Height H and characteristic width λ) combined with magnetic and gravity data have indirectly quantified the temporal evolution of this ridge-crest system. Our most robust result is that abyssal hills formed during slower spreading periods (ages > 8 Ma; full rates 36-44 mm/yr) are 31-86% taller and 21 ->100%, wider than hills created during the faster spreading interval (ages < 4 Ma; full rates 52-63 mm/yr). This study documents a well-resolved negative correlation between abyssal hill size parameters and full spreading rates for the Pacific-Antarctic ridge at 65° S. We also show evidence for a well-resolved positive correlation between H and λ which is expected to develop if abyssal hills are formed either by extensional tectonics or by constructional volcanism. Such positive correlation is mom consistent with abyssal hills created at slow-spreading ridges than those created at fast-spreading ridges [Goff, 1991].

The negative relationship between crustal thickness and abyssal hill size demonstrated in previous studies for slow-spreading rates cannot be systematically supported by this study. Variations in H and λ that cannot be explained in terms of either the spreading rate or crustal thickness effect include: (1) the anomalous] y large abyssal hills found along the northern-segment flowlines for 4-6 Ma age crust, where indication of crustal thinning is only seen for the Antarctic plate; (2) abyssal hill size estimates for crustal ages greater than 8 Ma are significantly higher for the Antarctic plate relative to the Pacific plate despite no significant asymmetry in half spreading rate and mantle Bouguer gravity anomaly; and (3) a 27-68% increase in abyssal hill height is observed close to the fracture zone for all subareas while either no significant changes (to the north of the PFZ) or up to a 40% decrease (to the south of the PFZ) in characteristic width estimates are found; these observations may reflect along-axis changes in either the amount of extension (without a corresponding variation in the strength of the lithosphere) or in the relative contribution of constructional volcanism to overall abyssal hill morphology.

The topographic roughness predictions due to normal faulting presented in Malinverno and Cowie [1993] provide a means of interpreting abyssal hill height and characteristic width characteristics in terms of lithospheric strength. Using their formulation for the dependence of the roughness due to normal faulting on profile length, it can be postulated that flexural length scale for the southern segment is in average larger than for the northern segment (i.e., the lithosphere is stronger to the south of the fracture zone).

Previous studies at slow-spreading ridges suggest the presence of both crustal thickness and abyssal hill size asymmetries between inside and outside corner crust generated near a ridge discontinuity [e.g., Tucholke et al., 1992]. For the slower spreading intervals of this flowline corridor (age >8 Ma) the abyssal hill size asymmetry seen is in the opposite sense to that predicted by differential crustal thickness; furthermore there is no apparent asymmetry in crustal thickness. Conversely, for the faster spreading periods (crustal age < 4 Ma), some asymmetry in crustal structure exists (though variable and likely related to volcanic overprinting), but no asymmetry in abyssal hill morphology can be detected. In this aspect, abyssal hills within the study area are more consistent with those generated at fast-spreading ridges (i.e., no systematic inside/outside comer asymmetry) rather than those generated at slow-spreading ridges. When comparing this conclusion to the opposite one noted above for the positive correlation between H and λ, wc find that these intermediate-spreading rate abyssal hills can be classified with neither the fast-spreading nor slow-spreading examples but require their own classification.

Acknowledgments.

We wish to thank the captain and crew of the R/V Maurice Ewing for their dedication and hard work in collecting this data, S. O'Hara and D. Chayes for Hydrosweep data reduction and S. Tebbens, D. Mueller, B. O'Brien and M. Wilkinson for assistance at sea. This research was supported by NSF grant XXX-XXXX. A portion of this research (C.A.R) was performed at the Jet Propulsion Laboratory, California Institute of Technology and was sponsored by NSF and NASA. We benefited from helpful reviews by X and Y. LDEO contribution number ZZZZ.

REFERENCES

Bicknell, J. D., J. - C. Sempere, K. C. Macdonald and P. J. Fox, Tectonics of a fast spreading center: A Deep-Tow and Sea Beam survey on the East Pacific Rise at 19030'S, Mar. Geophys. Res., 9,25-45, 1987.

Carbotte, S. and K. C. Macdonald, Comparison of seafloor fabric created at intermediate fast and ultra-fast spreading ridges, Eos, Trans. AGU, 72,456, 1991.

Cande, S. C., C. A. Raymond, W. F. Haxby, W. B. F. Ryan, S. Tebbens, S. O'Hara, D. Mueller, B. O'Brien and W. Wilkinson, Preliminary results of a Hydrosweep swath bathymetry, magnetics and gravity survey of a Pacific-Antarctic ridge FZ, Part I: Plate kinematics, Eos Trans. AGU, 73, 295, 1992.

Cande, S. C. and D. V. Kent, A geomagnetic polarity time scale for the late Cretaceous and Cenozoic, J. Geophys. Res., 97, 13917-13951, 1992

Chen, Y. and W. J. Morgan, Rift valley/no rift valley at mid-ocean ridges, J. Geophys. Res., 95, 17571-17581, 1990.

Edwards, M. H., W. B. F. Ryan and D. J. Fornari, A tectonic-volcanic model for abyssal hill formation on the intermediate-fas(spreading East Pacific Rise, Eos Trans. AGU, 73, 502, 1992.

Fornari, D., J. Gallo, M. H. Edwards, J. A. Madsen, J. A. Permit and A. N. Shor, Structure and Topography of the Siqueiros Transform Fault System: Evidence for the Development of Intra-Transform Fault System, Mar. Geophys. Res., 11,239-262, 1989.

Forsyth, D. J., Finite extension and low-angle normal faulting, Geology, 20,27-30, 1992.

Goff, J. A. and T. H. Jordan, Stochastic modeling of seafloor morphology: Inversion of Sea Beam data for second-order statistics, J. Geophys. Res., 93, 13,589-13,608, 1988.

Goff, J. A., A global and regional stochastic analysis of near-ridge abyssal hill morphology, J. Geophys. Res., 96, 21713-21737, 1991.

Goff, J. A., Quantitative characterization of abyssal hill morphology along flowlines in the Atlantic ocean, J. Geophys. Res., 97, 9183-9202, 1992.

Goff, J. A., M. C. Kleinrock, J. Lin and B. E. Tucholke, Quantitative analysis of abyssal hill morphology within three segments: the west flank of the MAR 25°25'N-27°1 O' N and 0-30 Ma, Eos Transactions, AGU, 73, 538, 1992.

Goff, J. A. , A. Malinverno, D. J. Fornari and J. R. Cochran, Abyssal hill segmentation: quantitative analysis of the East Pacific Rise Flanks 7°S-90S, J. Geophys. Res., 98, 13851-13862, 1993.

Hayes, D. E. and K. A. Kane, The dependence of seafloor relief on spreading rate, Geophys. Res. Lett., 18, 1425-1428, 1991.

Harrison, C. G. and L. Stieltjes, Faulting within the median valley, Tectonophysics, 38, 137-144, 1977.

Haxby, W. F., C. A. Raymond, Cande, S. C., W. B. F. Ryan, S. Tebbens, S. O'Hara, D. Mueller, B. O'Brien and W. Wilkinson, Preliminary results of a Hydrosweep swath bathymetry, magnetics and gravity survey of a Pacific-Antarctic ridge FZ, Part 11: Crustal Structure, EOS Trans. AGU, 73, 278, 1992.

Kappel, E. S. and W. B. F. Ryan, Volcanic episodicity and a non-steady state relief valley along Northeast Pacific spreading centers: Evidences from Sea Marc I, J. Geophys. Res., 91, 13925-13940, 1986.

Keeley , C., W. B. F. Ryan, L.. Pratson and W. F. Haxby, Ridge flank flooding from a segment midpoint revealed from Hydrosweep data: East Pacific Rise 7°S to 9°S, Eos, Trans. AGU, 73, 554, 1992.

Kong, L. S. L., R. S. Dietrick, P. J. Fox, L. A. Mayer and W. B. F. Ryan, The morphology and tectonics of the Mark area from Sea Beam and Sea Marc I observations (Mid-Atlantic Ridge 23° N), Mar. Geophys. Res., 10,59-80, 1988.

Lewis, B. T. R., Periodicities in volcanism and longitudinal magma flow, on the East Pacific Rise at 23°N, Geophys. Res. Lett., 6,753-756, 1979.

Lin, J. , B. E. Tucholke, M. C. Kleinrock and J. A. Goff, Variations in crustal faulting and magmatic accretion along the mid-Atlantic ridge and off-axis: results from the western flank of the MAR at 25-27°N , Eos Trans. AGU, 73, 538, 1992.

Lonsdale, P., Structural geomorphology of a fast-spreading rise crest: The East Pacific Rise near 32°S, Mar. Geophys. Res., 3,251-293, 1977.

Macdonald, K. C. and T. Atwater, Evolution of rifted ocean ridges, Earth Planet. Sci. Lett., 39,319-327, 1978.

Macdonald, K. C., Mid-ocean ridges: finite scale tectonic, volcanic and hydrothermal processes within the plate boundary zone, Ann. Rev. Plan. Science, 39,319-327.,1982.

Macdonald, K. C., The crest of the Mid-Atlantic Ridge: Models for Crustal Generation Processes and Tectonics, in Vogt, P. R.. and Tucholke, B. E.. (eds), The Geology of North America, Volume M, The Western North Atlantic Region, Geological Society of America, Boulder, 51-68, 1986.

Malinverno, A., A simple method to estimate the fractal dimension of a self-affine series, Geophys. Res. Lett., 17, 1953-1956, 1990.

Malinverno, A., Inverse square-root dependence of mi(i-ocean ridge flank roughness on spreading rate, Nature, 352,58-60,1991.

Malinverno, A., Transition between a valley and a high at the axis of mid-ocean ridges, Geology, 21,639-642, 1993.

Malinverno, A. and P. A. Cowie, Normal faulting and the topographic roughness of mid-ocean ridge flanks, J. Geophys. Res., 98, 17921-17935, 1993.

Marks, K. M. and J. M. Stock, Variations in the ridge morphology and depth-age relationships on the Pacific-Antarctic ridge, J. Geophys. Res., 99, 531-541, 1994.

Menard, H. W., Seafloor spreading ,topography and the second layer, Science, i 57, 923-924, 1967.

Mutter, J. C. and J. A. Karson, Structural processes at slow-spreading ridges, Science, 257,627-634, 1992.

Palmer, J., J. - C. Sempere, D. M. Christie and J. Phipps Morgan, Morphology and Tectonics of the Australian-Antarctic Discordance between 123°E and 128°E, Mar. Geophys. Res., 15, 121-152, 1993.

Parker, R. L. The rapid calculation of potential anomalies, Geophys. J. R. Astr. Sot., 31, 447-455, 1973.

Phipps Morgan, J. and Y. J. Chen, The genesis of oceanic crust: magma injection, hydrothermal circulation and crustal flow, J. Geophys. Rcs., 98, 6283-6298, 1993.

Pockalny, R. A., R. S. Detrick and P. J. Fox, Morphology and tectonics of the Kane Transform from Sea Beam bathymetry data, J. Geophys. Res., 93,3179-3193, 1988.

Press, W. H., B. P. Flannery, S. A. Teukolsky and W. T.. Vetterling, Numerical Recipes in C, 735 pp, Cambridge University Press, New York, 1991.

Rea, D. K., Model for the formation of topographic features on the East Pacific Rise crest, Geology, 3, 77-80, 1975.

Ryan, W. B. F., C. A. Raymond, S. C. Cande, W. F. Haxby, S. Tebbens, S. O'Hara, D. Mueller, B. O'Brien and M. Wilkinson, Documentation of ridge-axis jumps on the Pacific-Antarctic spreading center, Eos Trans. AGU, 73, 295, 1992.

Shaw, P. R., Ridge segmentation, faulting and crustal thickness in the Atlantic ocean, Nature, 358, 490-493, 1992.

Small, C. and D. T. Sandwell, 1992, An analysis of ridge-axis gravity roughness and spreading rate, J. Geophys. Res., 97, 3235-3245, 1992.

Smith, D. K. and J. Cann, Hundreds of small volcanoes on the median valley floor of the Mid-Atlantic Ridge at 24°-30°N, Nature, 348, 152-155, 1990.

Tucholke, B. E.. and H. Shouten, Kane Fracture Zone, Mar. Geophys. Res. 10, 1-39, 1988.

Tucholke, B. E. and J. Lin, Detachment faulting and its relation to geological structure at first- and second-order offsets of slow-spreading ridges, Eos Trans. AGU, 73, 286, 1992.

Tucholke, B. E., J. Lin and M. C.. Kleinrock, Crustal structures of the western flank of the mid-Atlantic ridge at 25°25'N to 27"1O'N, Eos Transactions, AGU, 73, 286, 1992.

Wang, X. J. and J. R. Cochran, Isostasy and mantle flow on the East Pacific Rise crest, Eos Trans. AGU, 74, 296,1993.

FIGURE CAPTIONS

Fig. 1. Shaded free-air gravity map derived from Geosat/Seasat data for the SW Pacific Ocean. The rectangular box denotes the Ewing cruise 92-1 survey limits [to be added to the final figure].

Fig. 2. Color relief maps of the study area using the oblique Mercator projection (pole of projection is 69° N and 87° W): (a) Hydrosweep bathymetry using, (b) magnetic anomalies and (c) Mantle Bouguer gravity anomalies corrected for the lithospheric thermal structure. Shading simulates illumination from the northwest. The three subareas referred to in this study (Antarctic north, Pacific north and Pacific south) and isochrons based on the identification of magnetic anomalies are indicated in (a). The gravity effect of the bathymetry and assumed Moho relief (at a constant depth of 6 km) were calculated along the tracklines (method of Parker [1972]; 4 terms were retained) and then subtracted from the shipborne free-air gravity. The densities used for water, crust and mantle material are 1030, 2900 and 3300 kg/m^3 respectively. [the final figure will be colored and will have the color code for each map at the bottom; the subareas and isochrons will also be superimposed in (a)]

Fig. 3. Bathymetric profiles -600 km long extending to both sides of the ridge crest for the northern and southern segments. The dashed line indicates the 2750 m depth. The axial high to the south of the Pitman Fracture Zone deepens by ~300 m relative to the north of the PFZ.

Fig. 4. (a) Full spreading rates based on the magnetic anomaly identification [Cande et al., 1992] and the Cande and Kent [1992] geomagnetic polarity time scale. Half spreading rate avm-ages for flowlines to the north and south of the Pitman Fracture Zone are shown in (a) and (b) respectivel y.

Fig. 5. Estimated flowline variations in the RMS height H (a-c) and characteristic width λ (d-f) of abyssal hills for the three subareas. The estimates, obtained for 2-3 adjacent swaths, are shown as open dots with error bars denoting one standard deviation. The location of the locally "anomalous" seafloor fabric (4-6 Ma crustal age) is indicated.

Fig. 6. Weighted averages (binned at every 2 Ma) of (a) RMS height and (b) characteristic width as a function of full spreading rates for the three subareas. The estimates cor-responding to the locally "anomalous" seafloor fabric (4-6 Ma crustal age) are indicated. The weighted H and λ estimates averaged for the three subareas (regional averages) are shown as opened rectangles in (c) and (d) respectively. The averaged estimates obtained for swaths adjacent to the PFZ (-5 km

from its topographic trace) arc shown as open triangles, In all cases the locally “anomalous” seafloor fabric was left out from the regression analysis shown as a straight line.

Fig. 7. (a) Weighted averages (binned at every 2 Ma) of RMS. height against characteristic width. b) The weighted estimates averaged for the three subareas (regional values) arc shown as opened rectangles. The averaged estimates obtained for swaths adjacent to the PFZ (triangles) and clearly depart from the regional averages (squares). In all cases the locally “anomalous” seafloor fabric was included in the regression analysis shown as a straight line..

Fig. 8. Abyssal hill size parameters (a) RMS height and (b) characteristic width as a function of full spreading rates extracted from global study of near axis abyssal hill morphology by Goff [1991]. The abyssal hill size estimates plotted for Pacific-Antarctic ridge arc shown as filled circles and represent averages for the O-2 Ma (full rate -55 mm/yr) and for 10-12 Ma (full rates -39 mm/yr) time intervals. PR+AI, PC, PN and MAR refer to the Pacific-Rivera and Africa-India, Pacific-Cocos, Pacific-Nazca and Mid-Atlantic Ridge respectively.

Fig 9. Analysis of residual flowlines profiles (thermal cooling curve removed) ~1350 km long to the north and south of the PFZ (a) Topographic roughness measurements against window length obtained using the roughness-length method [Malinverno, 1990]. The predicted transition from a power law regime to a flat line occurs at window lengths of -62 km to the south of the PFZ (α -22 km; Tc -5.6 km) and ~31 km to the north of PFZ (cx -11 km; Tc -2.1 km). (b) Power spectra of the two profiles.

TABLE 1

Region	Age, Ma	Full Spreading Rate, mm/yr	H, m	σ, m	λ, km	σ, km
AN	o-2	54.9	91±10	10.0	3.1±0.5	0.1
	2-4	56.7	85±4	8.1	3.1±1.2	0.5
	4-6	58.5	144±19	4.5	4.9*1.1	0.5
	6-8	44.0	113±8	5.1	3.430.4	0.1
	8-10	39.7	170±21	13.0	6.741.5	0.7
	10-12	38.9	158±18	5.4	6.2±1 .3	1.4
PN	o-2	54.9	77±6	3.0	3.3±0.8	0.5
	2-4	56.7	82±5	2.1	4.0±0.9	1.0
	4-6	58.5	139±12	6.5	5.2±1.1	0.9
	6-8	44.0	115±12	4.0	4.5±0.9	0.2
	8-10	39.'?	130±14	14.0	4.9±1.1	1.1
	10-12	38.9	109±7	5.5	4.130.7	0.7
PS	0-2	54.9	100±7	7.0	4 .7*1.2	0.9
	2-4	56.7	97±11	11.0	6.0±2.5	2.5
	4-6	58.5	90±7	5.4	4.2±0.8	0.4
	6-8	44.0	123±17	5.0	7.8±2.1	0,8
	8-1o	39.7	131±17	13.5	7.492.0	0.6
	10-12	38.9	129±20	17.5	6.9±2.3	0.1
			Adjacent to the Pitman Fracture Zone			
AN	o-2	54.9	116±6	4.8	4±0.4	0.3
	2-4	56.7	143±11	11.0	3±0.5	0.5
PN	o-2	54.9	119±8	8.0	3.450.4	0.3
	2-4	56.7	126±15	15.0	4.1±0.5	0.5
PS	o-2	54.9	126±9	7.0	2.5±0.8	0.8
	2-4	56.7	124±9	6.0	3.6±0.8	1.0

Notation: AN, Antarctic plate to the north of the Pitman Fracture Zone; PN, Pacific plate to the north of the Pitman Fracture Zone; PS, Pacific plate to the south of the Pitman Fracture Zone.

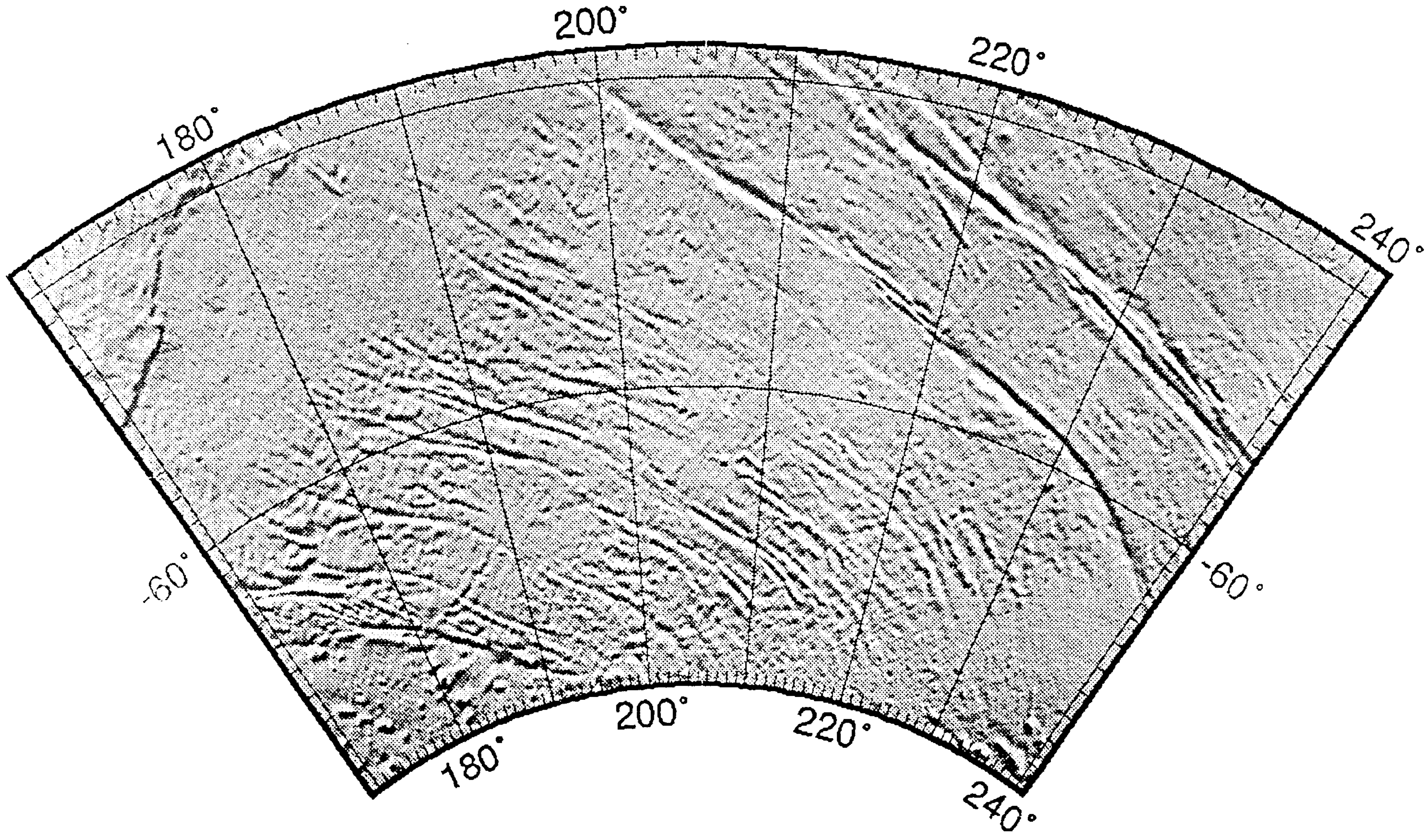
200°
220°
180°
240°
-60°
-60°
200°
220°
180°
240°

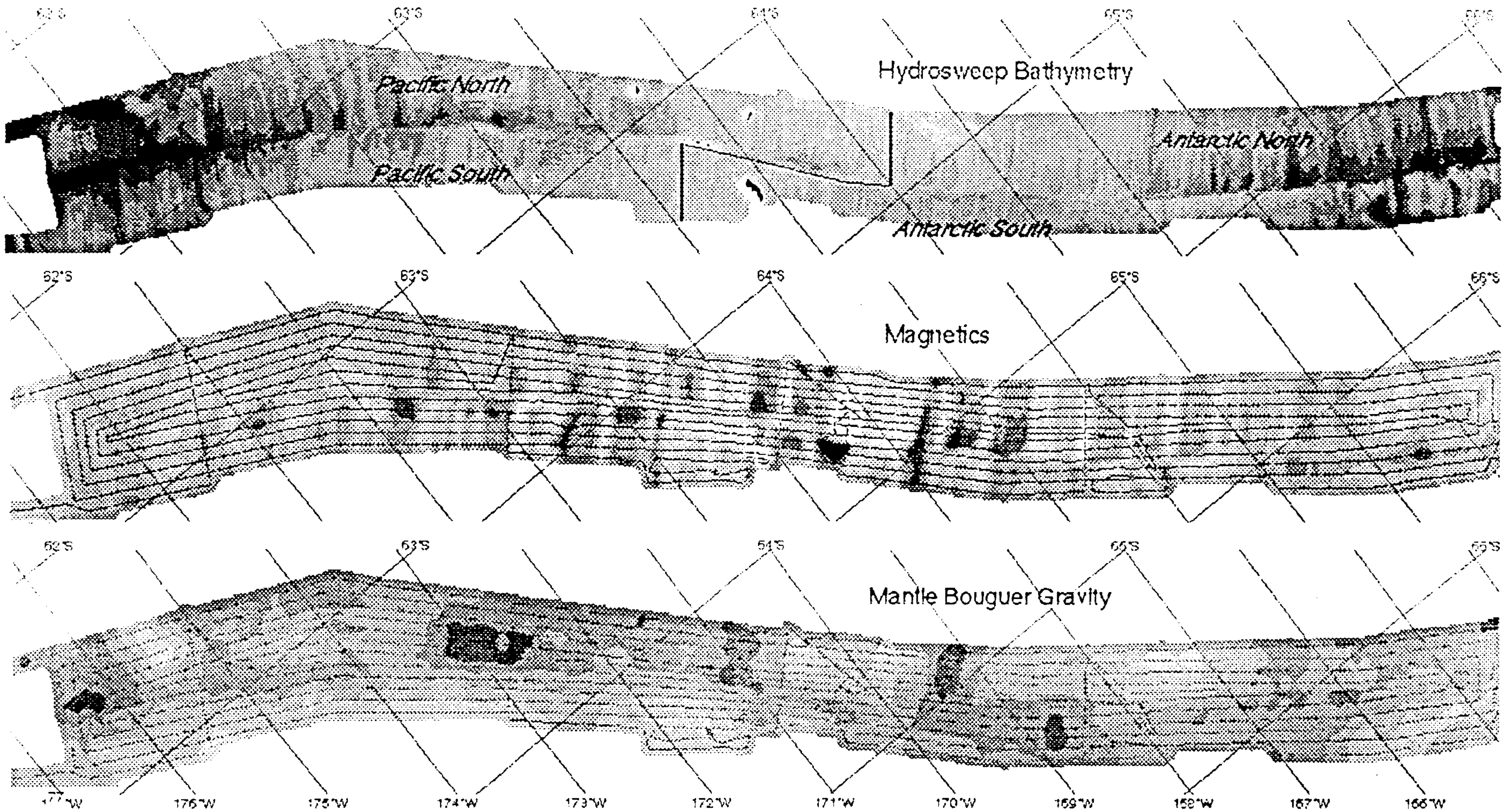
Hydrosweep Bathymetry
Pacific North
Pacific South
Antarctic North
Antarctic South
Magnetics
Mantle Bouguer Gravity
62°S
63°S
64°S
65°S
66°S
177°W
176°W
175°W
174°W
173°W
172°W
171°W
170°W
169°W
168°W
167°W
166°W

Fig. 2

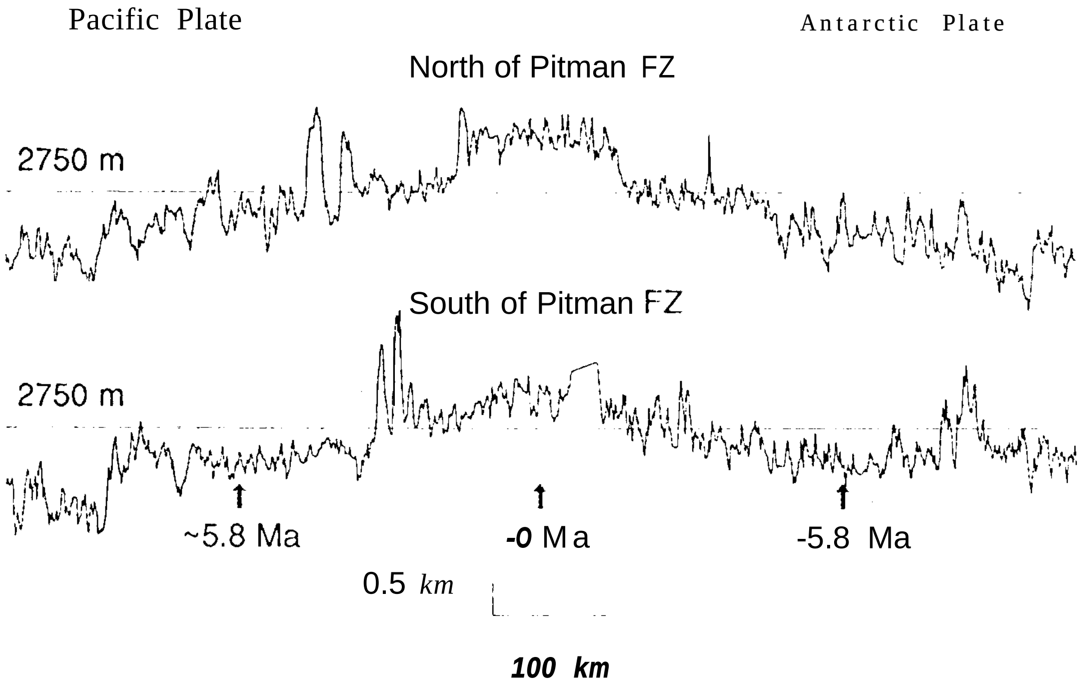

Pacific Plate
Antarctic Plate
North of Pitman FZ
2750 m
South of Pitman FZ
2750 m
~5.8 Ma
-0 Ma
-5.8 Ma
0.5 km
100 km

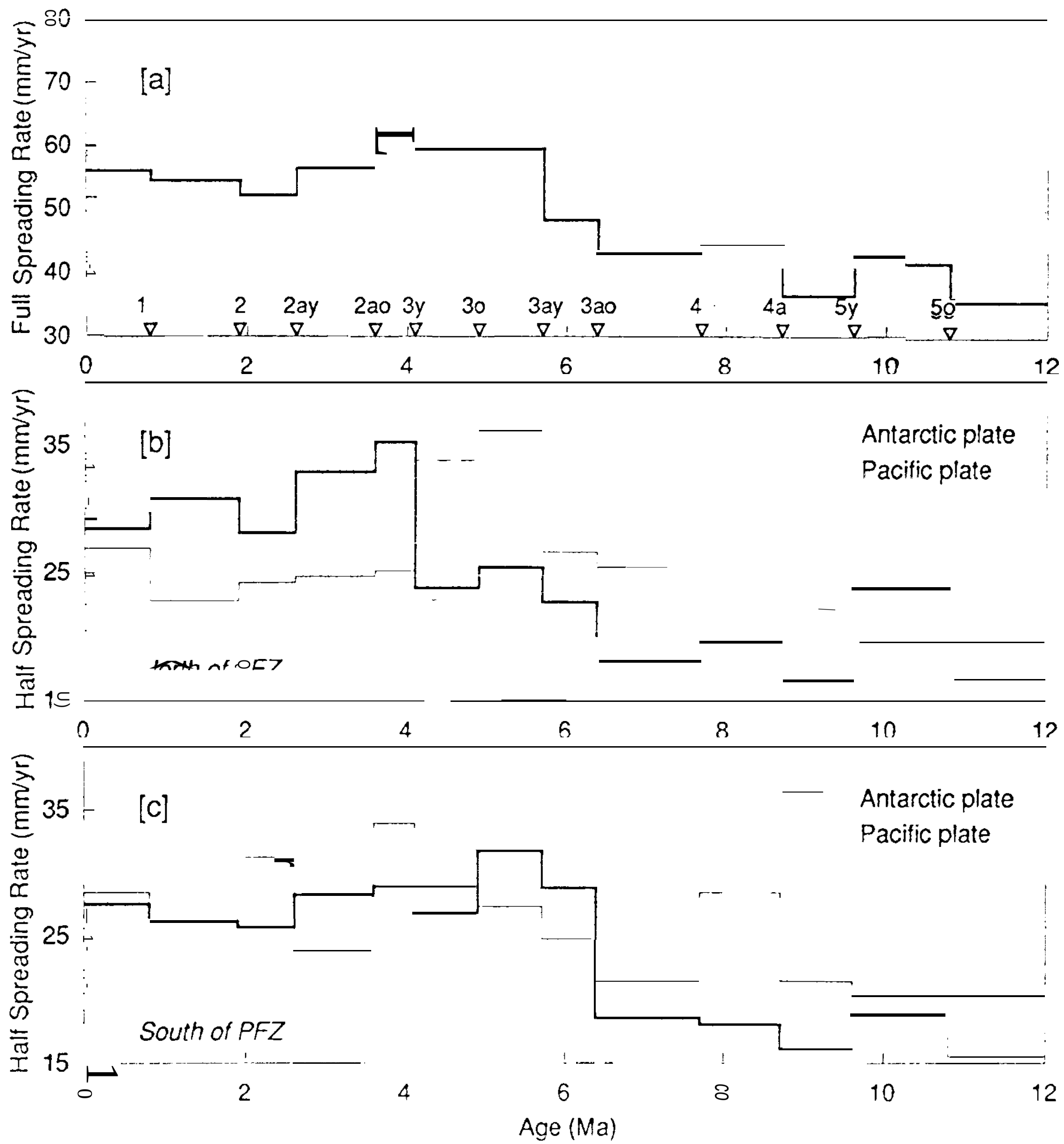

[a]
Full Spreading Rate (mm/yr)
1
2
2ay
2ao
3y
3o
3ay
3ao
4
4a
5y
5o
[b]
Half Spreading Rate (mm/yr)
Antarctic plate
Pacific plate
[c]
Half Spreading Rate (mm/yr)
Antarctic plate
Pacific plate
South of PFZ
Age (Ma)

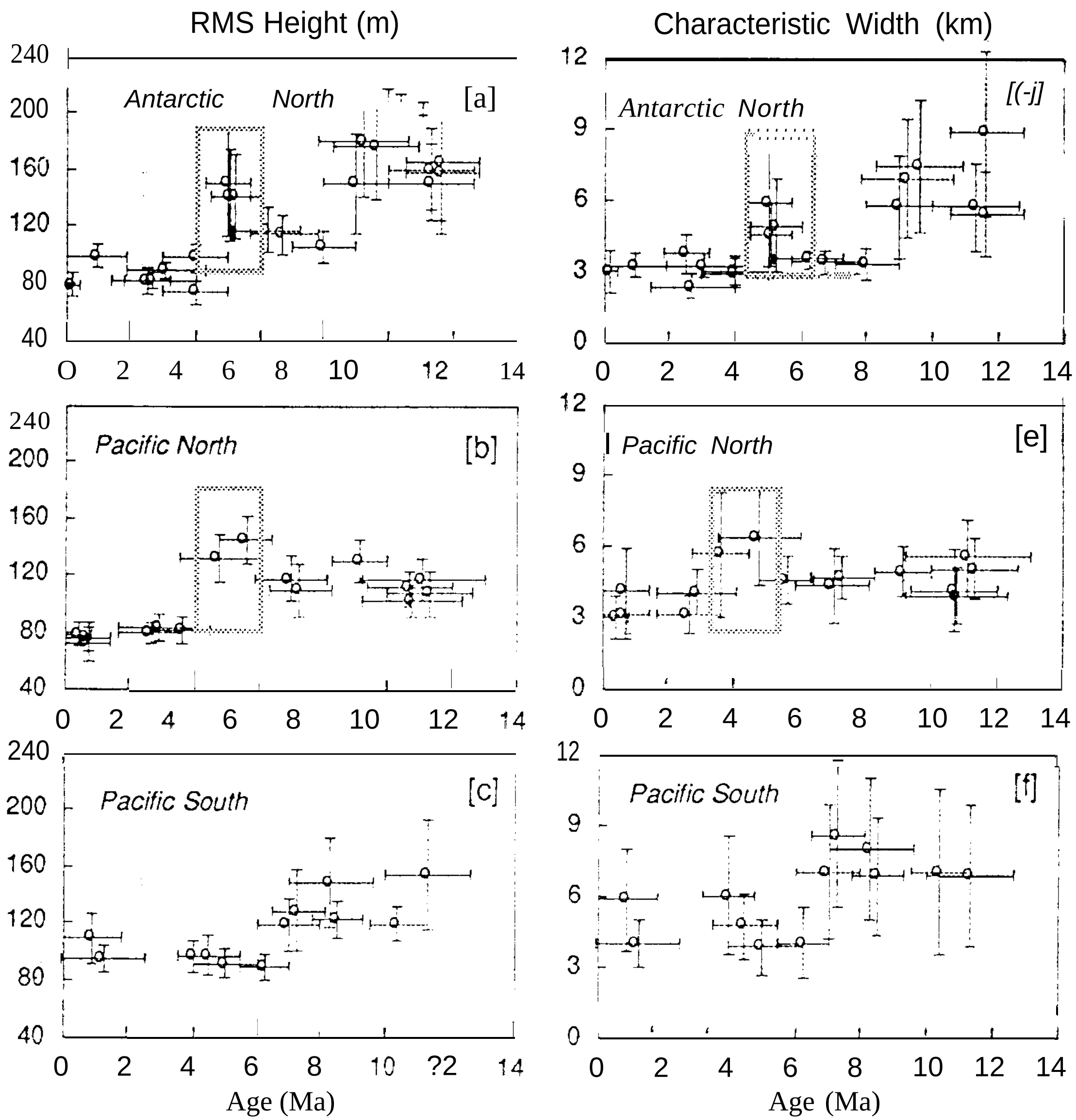
RMS Height (m)
Characteristic Width (km)
Antarctic North
[a]
Pacific North
[b]
Pacific South
[c]
[e]
[f]
Age (Ma)
Age (Ma)

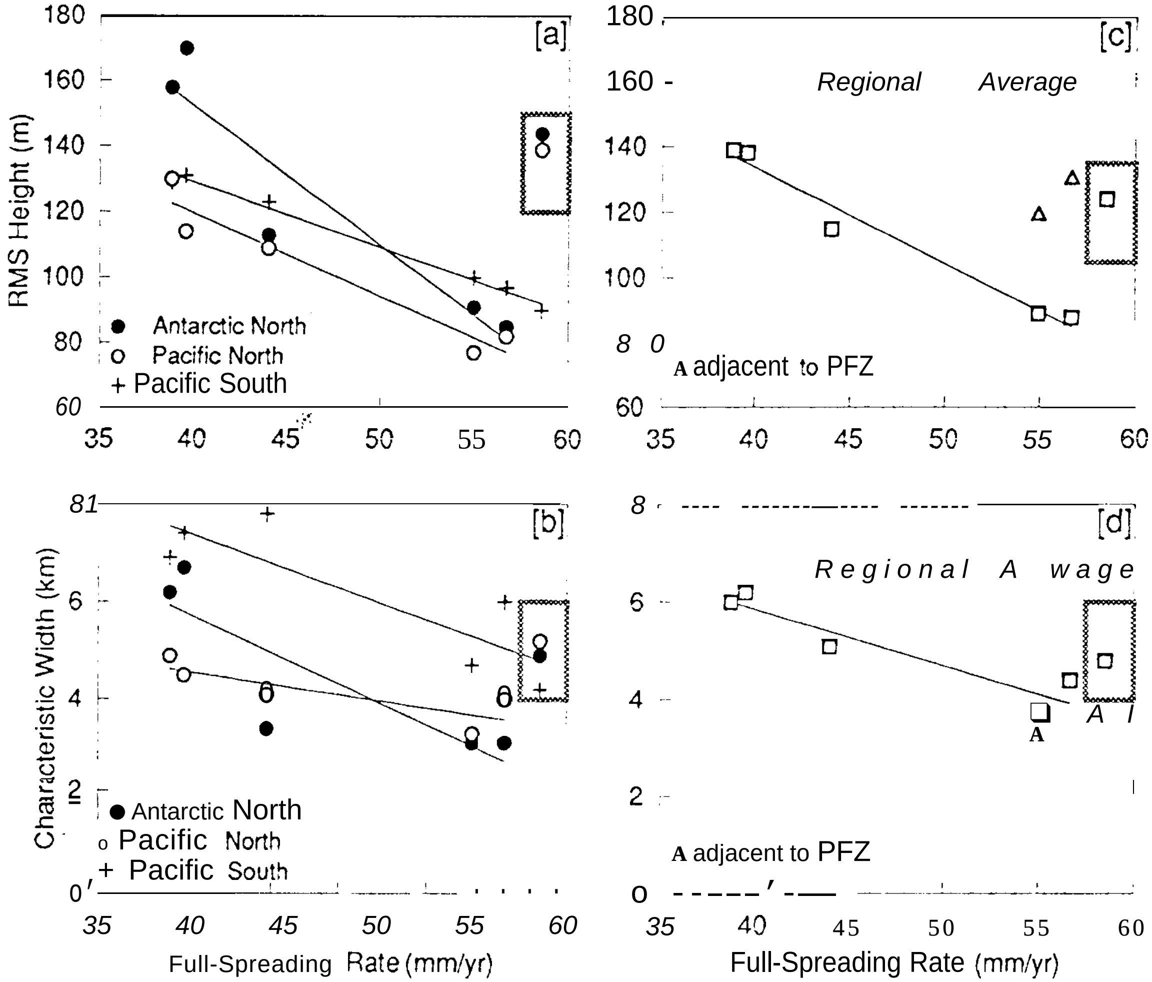

[a]
RMS Height (m)
Antarctic North
Pacific North
+ Pacific South
[c]
Regional Average
A adjacent to PFZ
[b]
Characteristic Width (km)
Antarctic North
Pacific North
+ Pacific South
Full-Spreading Rate (mm/yr)
[d]
Regional Average
A adjacent to PFZ
Full-Spreading Rate (mm/yr)

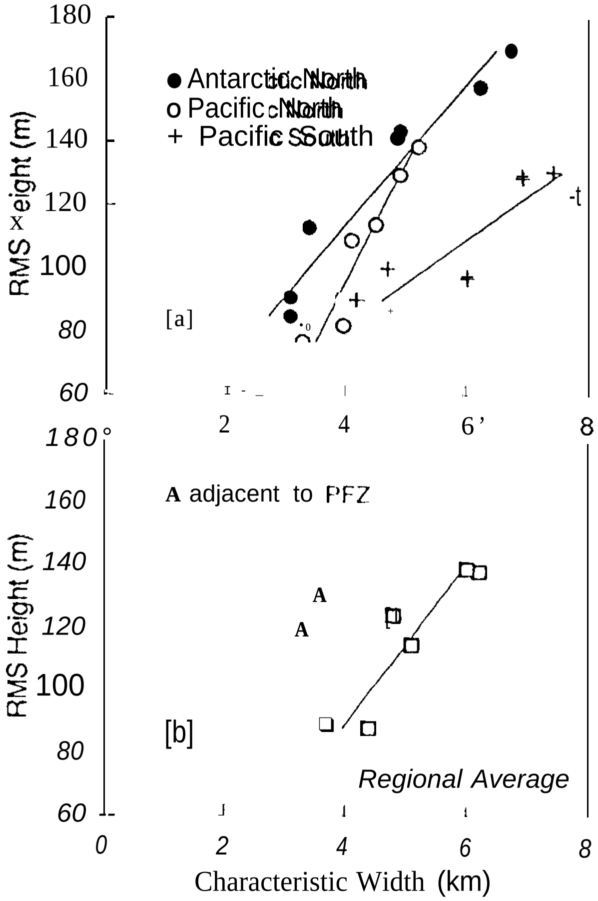
● Antarctic North
o Pacific North
+ Pacific South
[a]
RMS Height (m)
A adjacent to PFZ
[b]
Regional Average
RMS Height (m)
Characteristic Width (km)

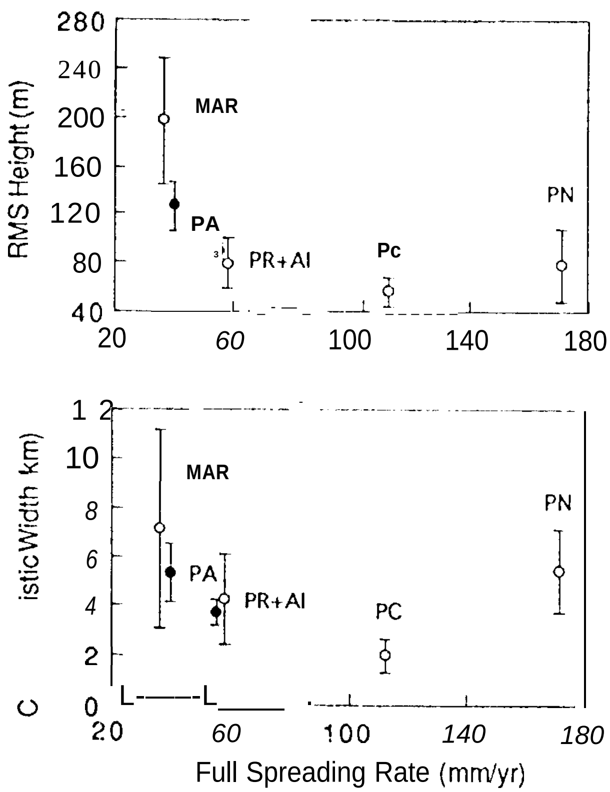

280
240
200
160
120
80
40
RMS Height (m)
MAR
PA
PR+AI
Pc
PN
20
60
100
140
180
12
10
8
6
4
2
0
isticWidth km)
C
MAR
PA
PR+AI
PC
PN
20
60
100
140
180
Full Spreading Rate (mm/yr)

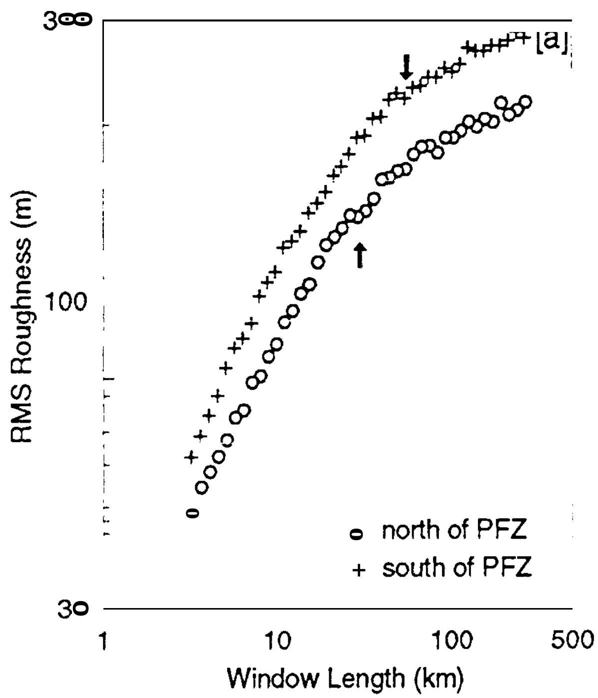

RMS Roughness (m)
300
100
30
1
10
100
500
Window Length (km)
[a]
north of PFZ
south of PFZ
Power Spectral Density (m^2.km)
1000000
100000
10000
1000
100
10
1
0.01
0.1
1
10
Wavenumber (1/km)
[b]
north of PFZ
south of PFZ